ISBN: 978-3-95450-234-9 ISSN: 2673-5504 doi:10.18429/JACoW-SRF2023-TUPTB006

MATERIALS DESIGN FOR SUPERCONDUCTING RF CAVITIES: ELECTROPLATING Sn, Zr, AND Au ONTO Nb AND CHEMICAL VAPOR DEPOSITION*

Z. Sun†, M. U. Liepe, T. Oseroff
Cornell Laboratory for Accelerator-Based Sciences and Education, Ithaca, NY, USA
Z. Baraissov, D. A. Muller
Applied and Engineering Physics, Cornell University, Ithaca, NY, USA
M. O. Thompson
Materials Science and Engineering, Cornell University, Ithaca, NY, USA

Abstract

Materials scientists seek to contribute to the development of next-generation superconducting radio-frequency (SRF) accelerating cavities. Here, we summarize our achievements and learnings, in designing advanced SRF materials and surfaces, . Our efforts involve electrochemical synthesis, phase transformation, and surface chemistry, which are closely coupled with superconducting properties, SRF performance, and engineering considerations. We develop electrochemical processes for Sn, Zr, and Au on the Nb surface, an essential step in our investigation for producing high-quality Nb_3Sn, ZrNb(CO), and Au/Nb structures. Additionally, we design a custom chemical vapor deposition system to offer additional growth options. Notably, we find the second-phase NbC formation in ZrNb(CO) and in ultra-high-vacuum baked or nitrogen-processed Nb. We also identify low-dielectric-loss ZrO_2 on Nb and NbZr(CO) surfaces. These advancements provide materials science approaches dealing with fundamental and technical challenges to build high-performance, multi-scale, robust SRF cavities for particle accelerators and quantum applications.

INTRODUCTION

Materials science becomes an integral part of multiple efforts in the development of next-generation superconducting radio-frequency (SRF) cavities, in designing advanced SRF materials and surfaces, including Nb_3Sn [1–3], ZrNb(CO) [4, 5], and Au/Nb surface design [6, 7], aiming to enable "bright beams" while reducing the size and cost of SRF systems [8–10]. We design advanced materials and surfaces guided by SRF performance metrics, which involve (i) achieving a suitably high critical temperature (T_c) to improve cryogenic cost and complexity, (ii) minimizing surface resistance (R_s) and maximizing quality factors (Q_0) to reduce power dissipation, and (iii) attaining a large superheating field (H_{sh}) and accelerating gradient (E_{acc}).

To explore and optimize SRF materials and surfaces, we employ a range of traditional strategies, including substitutional doping, light impurity processing and second-phase generation, surface passivation, and surface alloying. We have investigated Nb_3Sn [1–3], ZrNb(CO) [4, 5], Au/Nb [6], NbTiN/AlN/Nb [11, 12], V_3Si [13], thick-film Nb [14], and impurity-processed Nb [7]. We aim to bridge the gap between fundamental study and practical cavity production.

Electrochemical and chemical vapor depositions are our primary approaches and offer distinct advantages for SRF investigations due to their low cost, versatility, and reactivity. We have developed recipes and processes on the Nb surface for electroplating Sn for Nb_3Sn alloying, electroplating Zr for substitutional doping of Nb, and electroplating Au for fabricating Au/Nb surface structures.

Here, we review our progress and highlight the key findings. Further details can be accessed in other publications [1, 4, 6, 7]. We outline the fundamental and technical challenges associated with cavity production, with the aim of facilitating broader application and improved manufacturing of SRF cavities.

ELECTROPLATING Au ON Nb

Surface nanostructures on Nb, which involve native oxides, are crucial according to theoretical calculations [15, 16]. We have pursued two main directions. First, we have, to date, precisely established the structural profiles of the oxide regions at various depths, taking into account different baking and processing conditions [7]. Our findings indicate that the Nb surface region, comprising a combination of amorphous oxides and metallic components, is most likely normal conducting and impacts the superconducting bulk.

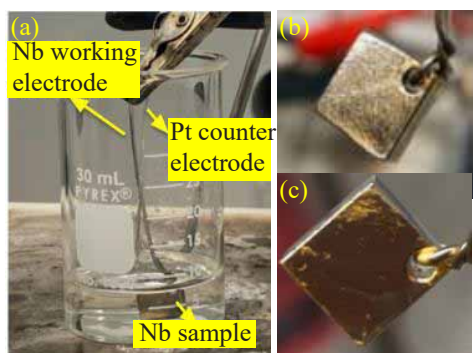

Figure 1: (a) Au electroplating setup. (b,c) Images showing Au film deposition on a Nb surface after different plating durations: (b) 60 s and (c) 600 s.

* Work supported by the U.S. National Science Foundation under Award PHY-1549132, the Center for Bright Beams.
† zs253@cornell.edu

ISBN: 978-3-95450-234-9 ISSN: 2673-5504 doi:10.18429/JACoW-SRF2023-TUPTB006

Secondly, we have designed a thin-Au/Nb SRF surface as a means to artificially replace surface oxides, leveraging the benefits of a proximity-coupled layer of normal-conducting Au [6]. The engineered subnanometer thickness and specific electrical properties of this Au layer have the potential to mitigate losses. We have demonstrated this process by employing physical vapor deposition on the Cornell sample host cavity that utilizes a plate sample.

To enable a viable transfer of this process to TESLA cavities, we assessed various custom processes and identified electroplating Au using the commercial Elevate gold 7990. This process was carried out *in situ* within an inert gas glovebox, ensuring oxygen and moisture levels were maintained below 0.5 ppm. Prior to deposition, Nb was immersed in a 2% HF solution to eliminate surface oxides.

We tested the Au electroplating process for Nb plates using a two-electrode system with Pt serving as the counter electrode, as depicted in Fig. 1a. Successful demonstrations of Au films were observed in Fig. 1b and 1c, corresponding to deposition times of 60 s and 600 s, respectively. The primary challenge is to achieve controlled deposition of subnanometer-thin Au films. In the initial attempt, we reduced the deposition time, while additional considerations will be addressed in future work.

ELECTROPLATING Zr ON Nb

We have demonstrated ZrNb(CO) films with high T_c under ambient pressure for SRF use [4, 5]. These films exhibit suitably high T_c values ranging from 9 – 13.5 K, and potentially up to 16 – 16.5 K, as indicated by flux expulsion. Such suitably high T_c values offer the potential to tune the coherence length and reduce sensitivity to material defects.

We first investigated the phase transformation and heat treatment using evaporated Zr-Nb thermal couples and identified 600 °C for 10 h as the optimum condition (to date). Furthermore, to produce SRF cavities, we developed a low-temperature (100 – 200 °C) electrochemical process using ZrF_4 in an ionic liquid and demonstrated this process using the Cornell sample test cavity, as shown in Fig. 2a. The SRF performance shows that BCS resistance trends lower than reference Nb, while quench fields occur at ~ 35 mT.

One particularly interesting observation is the presence of low-dielectric-loss ZrO_2 as the only surface oxide on Nb after Zr deposition or on ZrNb(CO) after thermal annealing, as exemplified in Fig. 2b. This oxide can serve as a dielectric passivation layer on existing Nb cavities and future ZrNb(CO) cavities.

The main challenge in this process is the incorporation of impurities. Zr is a gettering material, and we observed high concentrations of oxygen and carbon despite employing an inert gas glovebox with oxygen and moisture levels below 0.5 ppm and performing HF soaking to remove surface oxides prior to deposition. In the final ZrNb(CO) product, we observed the conversion of oxygen into ZrO_2 and the formation of rock-salt NbC (as exemplified in Fig. 3a). The presence of low-dielectric-loss ZrO_2 is beneficial, while the role of the second phase NbC remains unclear.

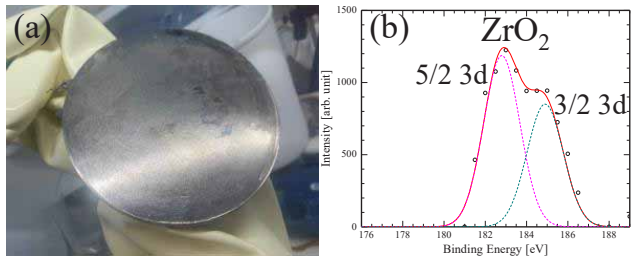

Figure 2: (a) Zr deposition (10 h) on the host plate of Cornell sample test cavity. (b) XPS spectra acquired from the ZrNb(CO) surface after 2 h deposition and subsequent annealing at 600 °C for 10 h, showing low-dielectric-loss ZrO_2.

SECOND PHASES: CARBIDE & SUBOXIDE

The presence of the second phase NbC is not only observed in ZrNb(CO) samples annealed at 600 °C (Fig. 3a) [4] but is also consistently observed in ultra-high-vacuum (UHV) baked and nitrogen-processed niobium at 120 – 800 °C (Fig. 3b) [7]. Our observations sufficiently challenge the concepts of nitrogen "doping" and oxygen "doping", as well as the explanations implied by these terms.

Our *in situ* baking and nitrogen processing experiments were conducted on electropolished Nb using the PHI Versaprobe X-ray photoelectron spectroscopy (XPS). High-resolution spectra were collected using a 100 μm monochromatic Al k-alpha X-ray (1486.6 eV) beam, with a 26 eV pass energy, a 50 ms/step, and up to 60 sweeps resulting in a high full-width-at-half-maximum resolution such as 0.3 – 0.6 eV for the Nb subpeaks.

During UHV or nitrogen baking, as exemplified in Fig. 3b, the characteristic peak was observed in over 350 spectra, and the inclusion of suboxide NbO_x was necessary to accurately fit over 375 spectra. Moreover, we found that carbide formation impacts the subsequent oxide formation during air exposure or low-temperature baking, irrespective of the gas environment. These processes modified the electron population profile, revealing the mechanistic involvement of second phases during baking and nitrogen processing [7].

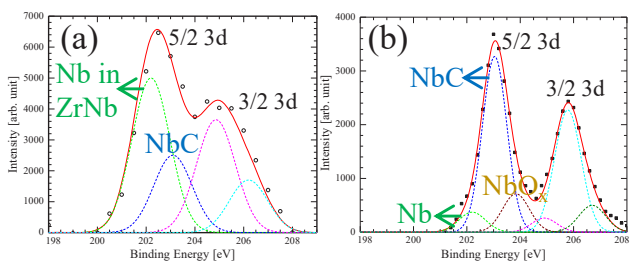

Figure 3: (a) XPS survey spectra acquired using the SSX-100 XPS instrument after 300 s of sputtering on ZrNb(CO) samples prepared through a 10 h electrochemical process, followed by annealing at 600 °C for 10 h. (b) High-resolution XPS spectra acquired *in situ* using the PHI Versaprobe XPS instrument after 18 s of sputtering on electropolished Nb samples at 500 °C under 7×10^{-11} Torr UHV baking.

ISBN: 978-3-95450-234-9 ISSN: 2673-5504 doi:10.18429/JACoW-SRF2023-TUPTB006

Our investigations [6, 7], combined with existing evidence from previous studies [17–19], strongly support that both surface oxides and second phase formation collectively contribute to the effects induced by UHV baking (or oxygen processing) and nitrogen processing.

ELECTROPLATING Sn ON Nb

We reported the progress of Sn seed-free electrochemical synthesis to produce Nb_3Sn on both sample-scale and a 3.9 GHz cavity at SRF'21 [2]. This approach offered three benefits: low surface roughness, improved stoichiometry, and high purity of electrochemical Nb_3Sn. Currently, we have successfully scaled up the process to produce a 1.3 GHz cavity and demonstrated ultra-low BCS resistance [1].

Figure 4a illustrates the custom setup employed for plating the 1.3 GHz cavity. To facilitate glovebox operation, we replaced the water bath heating system with wrapped fiberglass heating tape. We incorporated two thermocouples to monitor the plating temperature, which is a critical parameter for this process.

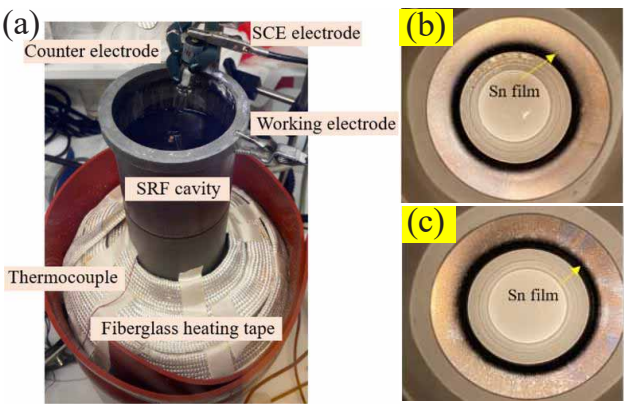

Figure 4: (a) Sn electroplating setup for a 1.3 GHz cavity. (b,c) Images showing Sn film deposition on the inner surface of the cavity (after HPR): (b) top side and (c) bottom side.

We observed the formation of perfect Sn films on the top side of the cavity, while the bottom side showed blue-colored spots. This suggests that operating large-volume plating solutions over an extended period of time requires further engineering considerations. Flipping over the cavity during the deposition process may work.

Additionally, these electrochemical Sn films survived high-pressure water rinsing (HPR), confirming their adherence to the cavity surface.

REMOTE PLASMA CHEMICAL VAPOR DEPOSITION SYSTEM

Since 2019, we have been designing and developing a remote plasma-enhanced chemical vapor deposition system tailored for SRF cavity production, as shown in Fig. 5. The cavity is loaded within a cleanroom environment. Four heating pipes allow the introduction of three precursors and carrier Ar gas into the system. The chemical vapor is regulated through calibrated mass flow controllers and a butterfly valve. A coil plasma generator is employed to provide the remote plasma. The deposition process takes place within a three-zone tube furnace capable of reaching temperatures up to 1200 °C, limited by the quartz tube. Exhaust safety is ensured through the integration of a cold trap and a high-volume dry pump. An additional turbo pump is incorporated to achieve vacuum conditions. The system is equipped with various monitoring tools, including a plasma analyzer, a residual gas analyzer, and a furnace controller, allowing for precise control of the heating profile and plasma monitoring throughout the deposition process. From 2021 on wards, G. Gaitan continues the system development [20].

CONCLUSION

- Building upon the success of the ultra-thin Au layer (artificially controlled normal conductor) passivated cavity with improved RF performance [6], we are developing Au electroplating processes for the fabrication of Au/Nb TESLA cavities.
- We have developed ZrNb(CO) alloys using electroplating (and evaporation), and demonstrated the first ZrNb(CO) cavity with improved BCS surface resistance and high T_c [4].
- We have demonstrated smooth, homogeneous, high-purity Nb_3Sn films using seed-free electrochemical synthesis and scaled up this process to produce a 1.3 GHz cavity with improved BCS resistance [1].
- We have identified the presence of low-loss-dielectric ZrO_2 on Nb and ZrNb(CO) surfaces [4].
- We have improved the fundamental understanding of vacuum baking and impurity processing in niobium, and highlighted the importance of considering second-phase formation in these processes [7].
- We have demonstrated several electrochemical processes as a viable deposition method for fabricating SRF cavities.
- We have designed a remote plasma-enhanced chemical vapor deposition system and initiated its development.
- We have identified several fundamental and technical challenges that need to be addressed in future work.

ACKNOWLEDGEMENTS

This work was supported by the U.S. National Science Foundation under Award PHY-1549132, the Center for Bright Beams. This work made use of the Cornell Center for Materials Research Shared Facilities which are supported through the NSF MRSEC program (DMR-1719875), and was performed in part at the Cornell NanoScale Facility, an NNCI member supported by NSF Grant NNCI-2025233. Z.S. thanks Dr. D. K. Dare, C. A. Dukes, A. Holic, J. Sears, G. Kulina, P. D. Bishop, H. G. Conklin, and T. M. Gruber for assisting in experiments and electrochemical and chemical vapor system installation.

ISBN: 978-3-95450-234-9 ISSN: 2673-5504 doi:10.18429/JACoW-SRF2023-TUPTB006

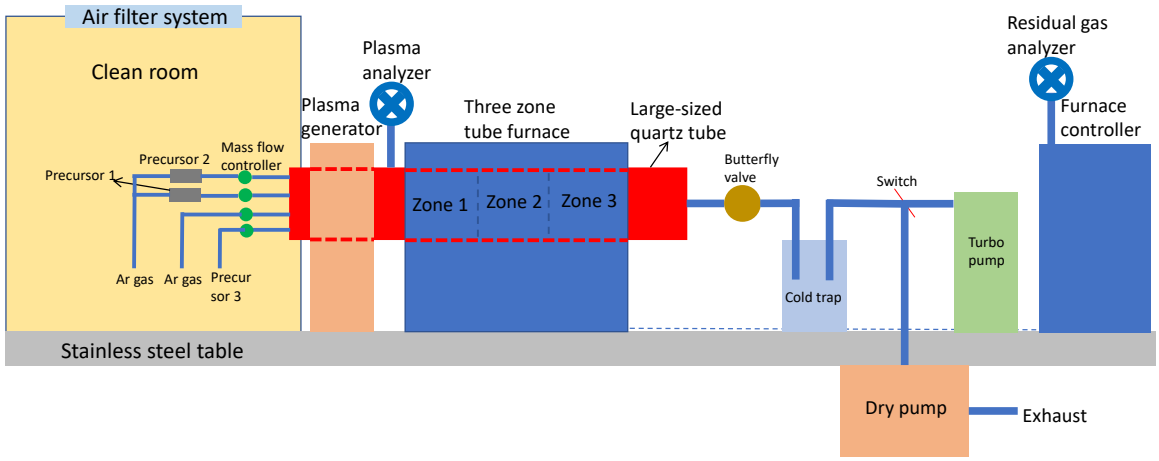

Figure 5: Sketch of a remote plasma chemical vapor deposition system.

REFERENCES

[1] Z. Sun *et al.*, "Smooth, homogeneous, high-purity Nb_3Sn superconducting RF resonant cavity by seed-free electrochemical synthesis", *arXiv*, 2023. doi:10.48550/arXiv.2302.02054

[2] Z. Sun *et al.*, "Toward stoichiometric and low-surface-roughness Nb_3Sn thin films via direct electrochemical deposition", in *Proc. SRF'21*, East Lansing, MI, USA, Jun.-Jul. 2021, pp. 710. doi:10.18429/JACoW-SRF2021-WEOTEV03

[3] Z. Sun *et al.*, "Thermodynamic route of Nb_3Sn nucleation: Role of oxygen", *arXiv*, 2023. doi:10.48550/arXiv.2305.05114

[4] Z. Sun *et al.*, "ZrNb(CO) RF Superconducting Thin Film with High Critical Temperature in the Theoretical Limit", *Adv. Electron. Mater.*, 2023. doi:10.1002/aelm.202300151

[5] Z. Sun *et al.*, "First Demonstration of a ZrNb Alloyed Surface for Superconducting Radio-Frequency Cavities", in *Proc. NAPAC'22*, Albuquerque, NM, USA, Aug. 2022, pp. 881–884. doi:10.18429/JACoW-NAPAC2022-THYE6

[6] T. Oseroff *et al.*, "Measurements of the amplitude-dependent microwave surface resistance of a proximity-coupled Au/Nb bilayer", *arXiv*, 2023. doi:10.48550/arXiv.2305.12035

[7] Z. Sun *et al.*, "Surface oxides, carbides, and impurities on RF superconducting Nb and Nb_3Sn: A comprehensive analysis", *arXiv*, 2023. doi:10.48550/arXiv.2305.02467

[8] N. A. Stilin *et al.*, "RF and thermal studies on conduction cooled Nb_3Sn SRF cavity", *Eng. Res. Express.*, vol. 5, p. 025078, 2023. doi:10.1088/2631-8695/acdd51

[9] A. Valente-Feliciano, "Superconducting RF materials other than bulk niobium: a review", *Supercond. Sci. Technol.*, vol. 29, p. 113002, 2016. doi:10.1088/0953-2048/29/11/113002

[10] T. E. Oseroff, M. Liepe, and Z. Sun, "Sample test systems for next-gen SRF surface", in *Proc. SRF'21*, East Lansing, MI, USA, Jun.-Jul. 2021, pp. 357. doi:10.18429/JACoW-SRF2021-TUOFDV07

[11] Z. Sun, M. Liepe, T. E. Oseroff, and X. Deng, "Characterization of Atomic-Layer-Deposited NbTiN and NbTiN/AlN Films for SIS Multilayer Structures", in *Proc. SRF'21*, East Lansing, MI, USA, Jun.-Jul. 2021, pp. 662. doi:10.18429/JACoW-SRF2021-WEPTEV012

[12] T. Oseroff *et al.*, "RF characterization of novel superconducting materials and multilayers", in *Proc. SRF'19*, Dresden, Germany, Jun.-Jul. 2019, pp. 950–955. doi:10.18429/JACoW-SRF2019-THP044

[13] K. Howard *et al.*, "Thermal annealing of sputtered Nb_3Sn and V_3Si thin films for superconducting radio-frequency cavities", *arXiv*, 2023. doi:10.48550/arXiv.2301.00756

[14] Z. Sun *et al.*, "Electrochemical polishing of chemical vapor deposited niobium thin films", *Thin Solid Films*, vol. 780, p. 139948, 2023. doi:10.1016/j.tsf.2023.139948

[15] T. Kubo and A. Gurevich, "Field-dependent nonlinear surface resistance and its optimization by surface nanostructuring in superconductors", *Phys. Rev. B*, vol. 100, p. 064522, 2019. doi:10.1103/PhysRevB.100.064522

[16] A. Gurevich and T. Kubo, "Surface impedance and optimum surface resistance of a superconductor with an imperfect surface", *Phys. Rev. B*, vol. 96, p. 184515, 2017. doi:10.1103/PhysRevB.96.184515

[17] G. D. L. Semione *et al.*, "Niobium near-surface composition during nitrogen infusion relevant for superconducting radio-frequency cavities", *Phys. Rev. Accel. Beams*, vol. 22, p. 103102, 2019. doi:/10.1103/PhysRevAccelBeams.22.103102

[18] E. M. Lechner *et al.*, "Electron tunneling and X-ray photoelectron spectroscopy studies of the superconducting properties of nitrogen-doped niobium resonator cavities", *Phys. Rev. Appl.*, vol. 13, p. 044044, 2020. doi:10.1103/PhysRevApplied.13.044044

[19] M. Delheusy *et al.*, "X-ray investigation of subsurface interstitial oxygen at Nb/oxide interfaces", *Appl. Phys. Lett.*, vol. 92, p. 101911, 2008. doi:10.1063/1.2889474

[20] G. Gaitan *et al.*, "Development of a CVD system for next-generation SRF cavities", in *Proc. NAPAC'22*, Albuquerque, NM, USA, Aug. 2022, pp. 372–374. doi:10.18429/JACoW-NAPAC2022-TUPA15